JACS
JOURNAL OF THE AMERICAN CHEMICAL SOCIETY

Communication

pubs.acs.org/JACS

Controllable Synthesis of Submillimeter Single-Crystal Monolayer Graphene Domains on Copper Foils by Suppressing Nucleation

Hong Wang,[†] Guanzhong Wang,*[,†] Pengfei Bao,[†] Shaolin Yang,[†] Wei Zhu,[†] Xing Xie,[‡] and Wen-Jun Zhang[‡]

[†]Hefei National Laboratory for Physical Sciences at Microscale, and Department of Physics, University of Science and Technology of China, Hefei, Anhui, 230026, P. R. China

[‡]Center of Super-Diamond and Advanced Films (COSDAF), and Department of Physics and Materials Science, City University of Hong Kong, Hong Kong SAR, P. R. China

Supporting Information

ABSTRACT: Submillimeter single-crystal monolayer and multilayer graphene domains were prepared by an atmospheric pressure chemical vapor deposition method with suppressing nucleation on copper foils through an annealing procedure. A facile oxidation visualization method was applied to study the nucleation density and morphology of graphene domains on copper foils. Scanning electron microscopy, transmission electron microscopy, atomic force microscopy, polarized optical microscopy, and Raman spectra showed that the submillimeter graphene domains were monolayer single crystals.

The novel properties[1,2] and the promising applications[3−5] have motivated increasing attempts to synthesize high quality graphene films since the monolayer graphene was prepared.[6−8] Large area uniform graphene films have been prepared on Cu substrates by chemical vapor deposition (CVD).[9,10] Recently, various shapes of single-crystal graphene domains such as hexagonal[11−13] and rectangular[14,15] shapes have attracted a lot of research interest, but the domain size was usually limited to tens of micrometers. Due to large numbers of graphene nucleation at the early stages and a very fast growth and mergence rate with the traditional CVD method, one can only obtain micrometer-size individual single-crystal domains or large area polycrystalline films.[16] The domain boundaries and rotational disorders[17,18] in the two-dimensional crystals are proven obstacles to electron transport.[12] Thus, it is desirable to prepare large-size high quality single-crystal graphene, which brings attention to the precise growth mechanism of graphene on a metal substrate. Although graphene grows from a nucleus, across steps and grain boundaries on metal substrates, and forms a graphene crystal domain, graphene crystals grown from different nuclei without an orientation relation can only coalesce to polycrystalline films. Therefore, reducing the nucleation density is a feasible route to prepare large-size single-crystal graphene domains. Li et al.[19] employed a copper-foil enclosure to synthesize large single-crystal graphene. However, it is still a challenge to control the nucleation stage for growth of supersized graphene single crystals.[20]

Here we report the growth of large monolayer single-crystal graphene domains with a notable suppression of graphene nucleation on copper foils by pregrowth longtime annealing. Graphene domains were synthesized on copper foils by atmospheric pressure chemical vapor deposition (APCVD). Copper foils were first annealed at 1045 °C for 3 h under 300 standard cubic centimeters per minute (sccm) Ar and 50 sccm H_2, and then a mixture of 0.5 sccm CH_4 and 500 sccm H_2 was applied for graphene growth. After 15.5 min, CH_4 and H_2 were shut off and 1000 sccm Ar was introduced for 30 s. Finally, the substrates were cooled down from 1045 to 500 °C at a rate of 0.1 °C/s under 300 sccm Ar and 4 sccm H_2 (Figure S1 in the Supporting Information).

To make the graphene domains optically visible, the after-growth copper foils were oxidized in air for about 1 min at 200 °C by a heating platform. After this procedure, the graphene domain covered sites were well protected from oxidation[21] and appeared to be brighter dots over the darker oxidized copper by bare-eye observation (Figure 1a). Under an optical microscope

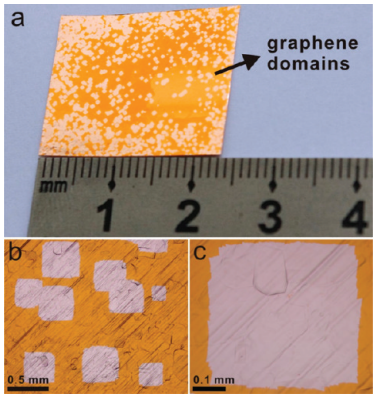

Figure 1. (a) Photo of the as-grown, separated graphene domains on Cu foil. (b, c) Optical microscopy images of the graphene domains in (a). The parallel dark stripes correspond to surface unevenness induced by mechanical processing of Cu foil.

(Figure 1b, c), the domains usually have a regular square shape with some jagged edges. Large domains were measured to be about 0.4 × 0.4 mm^2. Hexagonal shaped domains can also be prepared under the same growth conditions, but only these two

Received: November 11, 2011
Published: February 10, 2012

dx.doi.org/10.1021/ja2105976 | J. Am. Chem. Soc. 2012, 134, 3627−3630

shape domains were found in our samples. Recently, Wu et al. demonstrated that rectangular domains can only grow on Cu(111) while hexagonal domains can form on all other non-(111) Cu surfaces.[15]

We employed a large flow of H_2 to dilute CH_4 in the growth process. According to Li et al.,[16] low CH_4 concentration lead to a reduction of graphene nucleation. Our attempts also show that a high CH_4 concentration leads to the rapid growth of graphene over the Cu substrates, while highly diluted CH_4 reduces the growth rate and makes it more controllable in growing separated graphene domains (Figure S2). If only the CH_4 supply was shut off and the sample was cooled in a high concentration H_2 atmosphere (300 sccm Ar and 40 sccm H_2) after the growth stage, the graphene domains would appear to be etched into rectangular openings (Figure S3). Otherwise, no visible etching damage was observed on the sample cooled in a highly diluted H_2 atmosphere (300 sccm Ar and 4 sccm H_2) (Figure S4). In accordance with the copper-catalyzed etching mechanism proposed by Zhang et al. recently,[22] we believe that low concentration H_2 reduces the etch rate considerably and results in no significant etching damage.

The presence of impurities and defects on the surface of a substrate affects nucleation behavior very considerably.[23] They may act as active heteronuclei in the early stage of the graphene growth.[24] Gao et al.[25] demonstrated that the graphene nucleation rate near a step edge may be 10^4–10^7 times greater than that on a terrace due to a significantly lower nucleation barrier. At the center of some graphene domains, a spikelike structure was observed in SEM images (Figure 2e, S5) and was identified as impurities in the Cu substrate. It is suggested that several impurities which have a much lower nucleation barrier may act as heteronuclei at the early stage of the growth. High temperature substrate annealing is known to be helpful for the reduction of volatile impurities, contaminants, and defects on a copper surface, thus leading to the suppression of graphene nucleation. The influence of annealing and growth times on graphene nucleation density and domain size was studied. Figure 2a–c demonstrated that the graphene domain density decreases with prolonged annealing time. This indicates that a longer annealing time notably induces a reduction of nucleation density. Analogously, Figure 2d–f demonstrated that the domain size increases with prolonged growth time. It was about tens of micrometers with a growth time of 8 min (Figure 2d) and rapidly increased to about 100 and 350 μm with a growth time of 11 and 15.5 min (Figure 2e), respectively. The graphene domains started to merge if the growth time was extended further (Figure S6). On the other hand, graphene domains can hardly be observed for growth times less than 1 min under our growth conditions.

Figure 3a shows an optical micrograph of a square graphene domain transferred to a 300 nm SiO_2/Si substrate with Sun's method.[26] The high-magnification image of a corner of the domain is shown in Figure 3b. The uniform color contrast of the optical micrograph indicates that the film has excellent thickness uniformity. Atomic force microscopy (AFM) was employed to identify the number of layers of the sample. The height profile across a crack shows that the thickness of the graphene domain is about 0.6 nm, corresponding to a CVD derived monolayer graphene.[8]

Raman spectroscopy was used to evaluate the quality, thickness, and uniformity of the single-crystal graphene domains. Figure 4 shows Raman mapping of the D-band (Figure 4a), G-band (Figure 4b), and 2D-band (Figure 4c)

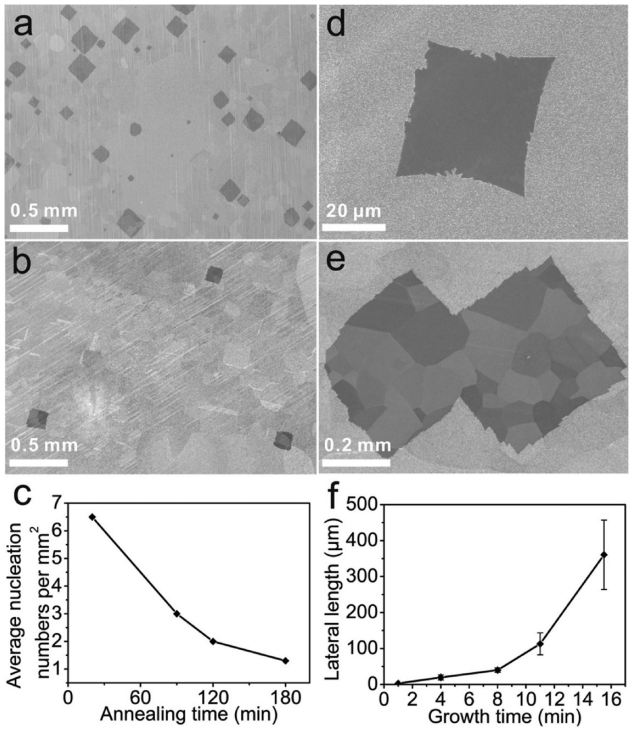

Figure 2. (a, b) SEM images of graphene domains on copper foils with different pregrowth annealing times (20 min and 3 h respectively). (c) The average graphene nucleation density with respect to annealing time. The growth time was 11 min in (a–c). (d, e) SEM images of graphene domains with different growth times (8 and 15.5 min respectively). The color contrast within a graphene domain represents different Cu grains after annealing, indicating that the graphene domain can grow continuously across Cu crystal grain boundaries. (f) The lateral length of the square domains as a function of the growth time. The annealing time in (d–f) was 3 h.

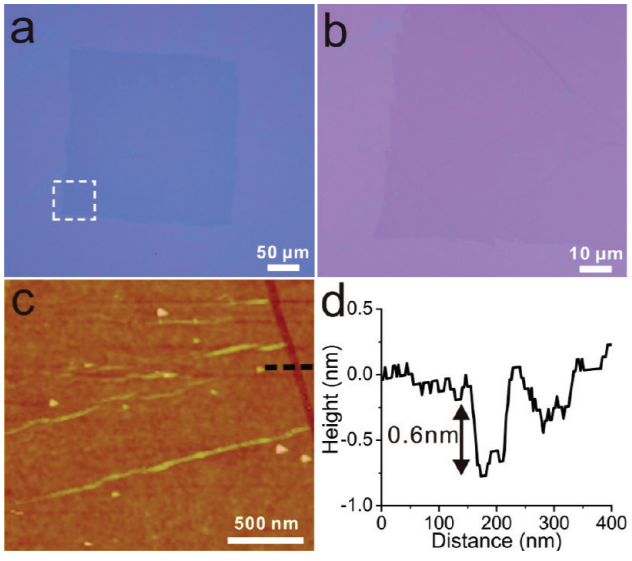

Figure 3. (a) Low, (b) high magnification optical microscopy and (c) AFM image of a square graphene domain transferred to SiO_2/Si substrate. (d) A height profile was taken from the position indicated in (c).

recorded at the corner area of a graphene domain. A typical Raman spectrum is displayed in Figure 4d, in which the G-peak (~1591 cm^{-1}) and 2D-peak (~2689 cm^{-1}) were shown. The

dx.doi.org/10.1021/ja2105976 | J. Am. Chem. Soc. 2012, 134, 3627–3630

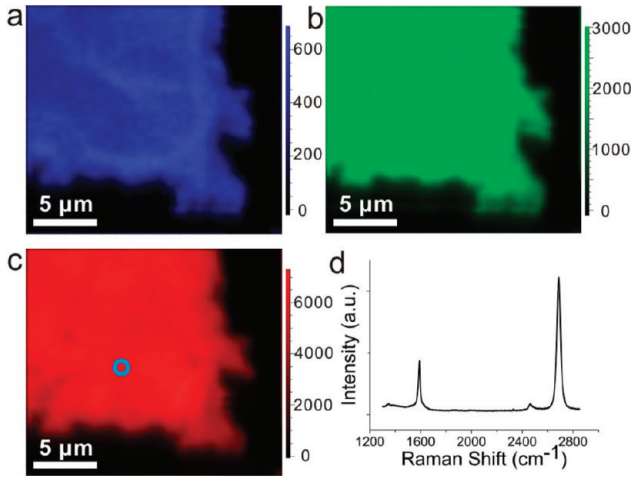

Figure 4. (a–c) D-band, G-band, and 2D-band Raman maps of a corner of a square-shaped graphene domain. (d) Raman spectra taken in the circled area shown in (c).

I_{2D}/I_G intensity ratio is about 3, and the full width at half-maximum (fwhm) of the 2D-peak is about 33 cm^{-1}. These results confirm that the graphene is monolayer. Furthermore, the disorder-induced D-peak (~1345 cm^{-1}) is very weak, indicating the high quality of the graphene film.

We also found other evidence that impurities served as nucleation centers in the growth of graphene domains. As shown in Figure 5a, a graphene domain with an impurity center

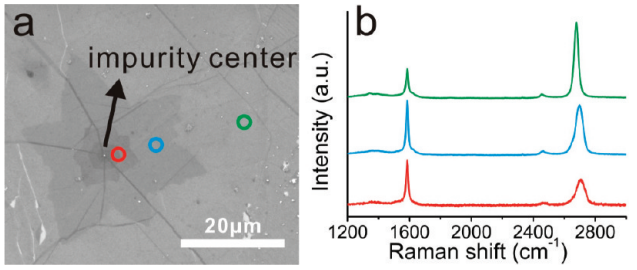

Figure 5. (a) SEM image of multinucleation in the center of a large graphene domain on SiO_2/Si substrate. The white areas are some cracks caused during the transfer process. (b) Raman spectra taken in the circled area shown in (a).

which appeared as a multinucleation site was transferred onto a SiO_2/Si substrate. This terraced structure of a few layers of graphene is similar to Robertson's result,[11] but with a much larger domain size. Raman spectra of different positions on the terraced structure are shown in Figure 5b. The green-circled area in the big graphene domain shows I_{2D}/I_G = 3 and fwhm (2D) = 33 cm^{-1}, which corresponds to a monolayer graphene, while the blue-circled (pink-circled) spot shows I_{2D}/I_G = 0.95 and fwhm (2D) = 60 cm^{-1} (I_{2D}/I_G = 0.58 and fwhm (2D) = 72 cm^{-1}), respectively, indicating increased graphene layers toward the center of the terraced structure.

Figure 6a shows a low magnification transmission electron microscopy (TEM) image of a corner in a square graphene domain (as marked by a white dashed line). Figure 6b shows a TEM image of a cracked area of the graphene domain. The high-resolution TEM image (Figure 6c) taken from the arrowed region marked in Figure 6b indicates the graphene domain is monolayer. To identify the crystallinity of the graphene domains, selected area electron diffraction (SAED)

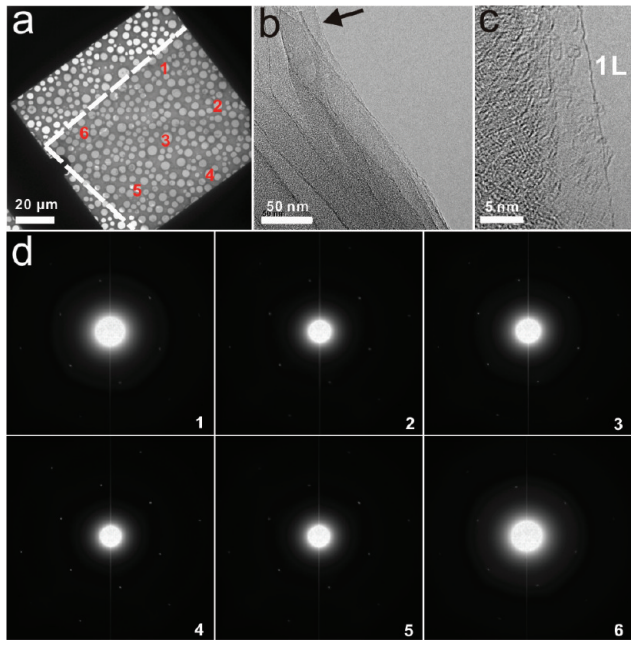

Figure 6. (a) Low magnification TEM image of a corner in a square graphene domain transferred to TEM grids. (b) TEM image of a cracked area on the graphene domain. (c) High-resolution TEM image taken from region marked with arrow in (b). (d) SAED of the six areas numbered in (a).

patterns were taken from six different sites of the graphene domain. As shown in Figure 6d, only one set of hexagonal diffraction spots without rotation was observed, revealing the detected area is a single crystalline film. SAED patterns recorded from other areas of the domain also displayed identical diffraction spots, indicating the whole graphene domain is a single crystalline film. In addition, we employed a direct domain visualization method[27] proposed by Kim et al. to confirm the crystallinity of the submillimeter graphene domains. Polarized optical microscopy (POM) images show similar colors within each graphene domain (Figure S7), indicating no domain boundaries in the submillimeter graphene domains.

It was also found that the cooling rate can significantly affect the layer numbers of graphene domains. High-quality monolayer graphene domains can only be obtained with low cooling rates, while high cooling rates result in multilayer graphene domains with more defects, as confirmed by Raman spectra. Bhaviripudi et al. also revealed that multilayer graphene can be obtained on copper foils by APCVD and the growth was not always self-limiting under APCVD conditions.[28] Thus, more research should be done to understand the precise mechanism of single-crystal graphene domain formation on copper foils by APCVD.

In conclusion, we have developed an annealing method to control the nucleation density of graphene on copper foils by APCVD and synthesized submillimeter-size graphene domains. A facile oxidation visualization method was applied to study the nucleation density and morphology of graphene domains on copper substrates. SEM, TEM (HRTEM and SAED), AFM, POM, and Raman spectra showed that a submillimeter graphene domain was a monolayer single crystal. Suppressing nucleation through an annealing procedure offers an effective way to grow large graphene single crystals.

dx.doi.org/10.1021/ja2105976 | J. Am. Chem. Soc. 2012, 134, 3627–3630

■ ASSOCIATED CONTENT

Supporting Information

Experimental procedures and additional figures. This material is available free of charge via the Internet at http://pubs.acs.org.

■ AUTHOR INFORMATION

Corresponding Author

gzwang@ustc.edu.cn

Notes

The authors declare no competing financial interest.

■ ACKNOWLEDGMENTS

We thank Dr. Lei Zhou and Dr. Xiaoshuang Shen for their help in the preparation of this paper and Mr Gongpu Li for his assistance in TEM experiments. This work was supported by the National Basic Research Program of China (2011CB921400, 2009CB939900) and the Natural Science Foundation of China (Grant No. 50772100).

■ REFERENCES

(1) Geim, A. K.; Novoselov, K. S. *Nat. Mater.* **2007**, *6*, 183.
(2) Castro Neto, A. H.; Guinea, F.; Peres, N. M. R.; Novoselov, K. S.; Geim, A. K. *Rev. Mod. Phys.* **2009**, *81*, 109.
(3) Wang, X.; Zhi, L.; Mullen, K. *Nano Lett.* **2007**, *8*, 323.
(4) Lin, Y.-M.; Dimitrakopoulos, C.; Jenkins, K. A.; Farmer, D. B.; Chiu, H.-Y.; Grill, A.; Avouris, P. *Science* **2010**, *327*, 662.
(5) Bonaccorso, F.; Sun, Z.; Hasan, T.; Ferrari, A. C. *Nat. Photonics* **2010**, *4*, 611.
(6) Berger, C.; Song, Z.; Li, X.; Wu, X.; Brown, N.; Naud, C.; Mayou, D.; Li, T.; Hass, J.; Marchenkov, A. N.; Conrad, E. H.; First, P. N.; de Heer, W. A. *Science* **2006**, *312*, 1191.
(7) Sutter, P. W.; Flege, J.-I.; Sutter, E. A. *Nat. Mater.* **2008**, *7*, 406.
(8) Reina, A.; Jia, X. T.; Ho, J.; Nezich, D.; Son, H. B.; Bulovic, V.; Dresselhaus, M. S.; Kong, J. *Nano Lett.* **2009**, *9*, 30.
(9) Li, X. S.; Cai, W. W.; An, J. H.; Kim, S.; Nah, J.; Yang, D. X.; Piner, R.; Velamakanni, A.; Jung, I.; Tutuc, E.; Banerjee, S. K.; Colombo, L.; Ruoff, R. S. *Science* **2009**, *324*, 1312.
(10) Levendorf, M. P.; Ruiz-Vargas, C. S.; Garg, S.; Park, J. *Nano Lett.* **2009**, *9*, 4479.
(11) Robertson, A. W.; Warner, J. H. *Nano Lett.* **2011**, *11*, 1182.
(12) Yu, Q.; et al. *Nat. Mater.* **2011**, *10*, 443.
(13) Wu, W.; Jauregui, L. A.; Su, Z.; Liu, Z.; Bao, J.; Chen, Y. P.; Yu, Q. *Adv. Mater.* **2011**, *23*, 4898.
(14) Liu, W.; Li, H.; Xu, C.; Khatami, Y.; Banerjee, K. *Carbon* **2011**, *49*, 4122.
(15) Wu, Y. A.; Robertson, A. W.; Schäffel, F.; Speller, S. C.; Warner, J. H. *Chem. Mater.* **2011**, *23*, 4543.
(16) Li, X.; Magnuson, C. W.; Venugopal, A.; An, J.; Suk, J. W.; Han, B.; Borysiak, M.; Cai, W.; Velamakanni, A.; Zhu, Y.; Fu, L.; Vogel, E. M.; Voelkl, E.; Colombo, L.; Ruoff, R. S. *Nano Lett.* **2010**, *10*, 4328.
(17) Kim, K.; Lee, Z.; Regan, W.; Kisielowski, C.; Crommie, M. F.; Zettl, A. *ACS Nano* **2011**, *5*, 2142.
(18) Huang, P. Y.; Ruiz-Vargas, C. S.; van der Zande, A. M.; Whitney, W. S.; Levendorf, M. P.; Kevek, J. W.; Garg, S.; Alden, J. S.; Hustedt, C. J.; Zhu, Y.; Park, J.; McEuen, P. L.; Muller, D. A. *Nature* **2011**, *469*, 389.
(19) Li, X.; Magnuson, C. W.; Venugopal, A.; Tromp, R. M.; Hannon, J. B.; Vogel, E. M.; Colombo, L.; Ruoff, R. S. *J. Am. Chem. Soc.* **2011**, *133*, 2816.
(20) Ajayan, P. M.; Yakobson, B. I. *Nat. Mater.* **2011**, *10*, 415.
(21) Chen, S.; Brown, L.; Levendorf, M.; Cai, W.; Ju, S.-Y.; Edgeworth, J.; Li, X.; Magnuson, C. W.; Velamakanni, A.; Piner, R. D.; Kang, J.; Park, J.; Ruoff, R. S. *ACS Nano* **2011**, *5*, 1321.
(22) Zhang, Y.; Li, Z.; Kim, P.; Zhang, L.; Zhou, C. *ACS Nano* **2012**, *6*, 126.
(23) Mullin, J. W. *Crystallization*, 3rd ed.; Butterworth Heinemann: London, 1993.
(24) Nie, S.; Wofford, J. M.; Bartelt, N. C.; Dubon, O. D.; McCarty, K. F. *Phys. Rev. B* **2011**, *84*, 155425.
(25) Gao, J.; Yip, J.; Zhao, J.; Yakobson, B. I.; Ding, F. *J. Am. Chem. Soc.* **2011**, *133*, 5009.
(26) Sun, Z.; Yan, Z.; Yao, J.; Beitler, E.; Zhu, Y.; Tour, J. M. *Nature* **2010**, *468*, 549.
(27) Kim, D. W.; Kim, Y. H.; Jeong, H. S.; Jung, H.-T. *Nat. Nanotechnol.* **2012**, *7*, 29.
(28) Bhaviripudi, S.; Jia, X.; Dresselhaus, M. S.; Kong, J. *Nano Lett.* **2010**, *10*, 4128.